Werk

Jahr: 1983
Kollektion: fid.geo
Signatur: 8 Z NAT 2148:52
Digitalisiert: Niedersächsische Staats- und Universitätsbibliothek Göttingen
Werk Id: PPN1015067948_0052
PURL: http://resolver.sub.uni-goettingen.de/purl?PPN1015067948_0052

LOG Id: LOG_0029
LOG Titel: Evidence for lamination in the lower continental crust beneath the Black Forest (Southwestern Germany)
LOG Typ: article

Übergeordnetes Werk

Werk Id: PPN1015067948
PURL: http://resolver.sub.uni-goettingen.de/purl?PPN1015067948
OPAC: http://opac.sub.uni-goettingen.de/DB=1/PPN?PPN=1015067948

Contact

Niedersächsische Staats- und Universitätsbibliothek Göttingen
Georg-August-Universität Göttingen
Platz der Göttinger Sieben 1
37073 Göttingen
Germany
Email: gdz@sub.uni-goettingen.de

J Geophys (1983) 52:109–118

Journal of Geophysics

Evidence for Lamination in the Lower Continental Crust Beneath the Black Forest (Southwestern Germany)

N. Deichmann and J. Ansorge
Institute of Geophysics, ETH-Hönggerberg, CH-8093 Zürich, Switzerland

Abstract. A 113 km long seismic refraction profile, with an average station spacing of 3 km, was recorded along the eastern margin of the Black Forest (southwestern Germany). Travel-times were modelled by ray-tracing, and amplitudes by a combination of reflectivity and asymptotic ray-theory methods. The resulting upper crustal model is characterized by a strong velocity gradient reaching 6.0 to 6.1 km/s at a depth between 8 and 10 km. Sedimentary reverberations are found to mask possible evidence for a discontinuity or a low-velocity layer in the middle crust, so that the existence of such a structure could not be demonstrated from this data alone. The reflections from the crust-mantle boundary consist of higher-frequency precursors and a lower-frequency main phase, followed by irregular reverberations. While the latter are probably due to multiple reflections and conversions within the sediments, the amplitudes and the frequency selective character of the former is best explained by a transition zone, between 20 and 26 km depth, consisting of a lamina-like sequence of velocity inversions.

Key words: Crustal structure – Refraction seismology – Synthetic seismograms – Velocity gradients – Low-velocity zone – Crust-mantle Transition

Introduction

The seismic refraction profile presented in this paper was recorded along the eastern margin of the Black Forest, southern Germany. It fills a gap between the intensively studied area of the southern Rhinegraben in the west (Mueller et al., 1969; Mueller et al., 1973; Edel et al., 1975; Prodehl et al., 1976), the area of the South German Molasse Basin in the east (Emter, 1971; 1976) and the recently investigated geothermal anomaly in the Suabian Jura, near Urach, to the northeast (Bartelsen et al., 1982; Jentsch et al., 1982).

Using both travel-time and amplitude information, it was possible to investigate the velocity gradient of the upper crystalline basement, the problem of the possible existence of a low-velocity layer in the upper or middle crust and the nature of the crust-mantle transition.

Offprint requests to: N. Deichmann

Contribution No. 403, Institute of Geophysics ETH Zürich, Switzerland

Geological Setting

The data were obtained between 1974 and 1980, along a north-south trending profile, from ten explosions in a single quarry near the town of Sulz am Neckar. As can be seen from the locations of the recording sites in Fig. 1, the first 90 km of this 113 km long line are situated along the edge of the crystalline Black Forest, where it dips beneath the Triassic sediments. Beyond 90 km, the line enters the Swiss Molasse Basin and crosses the eastern end of the Swiss Jura. From borehole data at Sulz and at other locations along the profile compiled in the geological literature

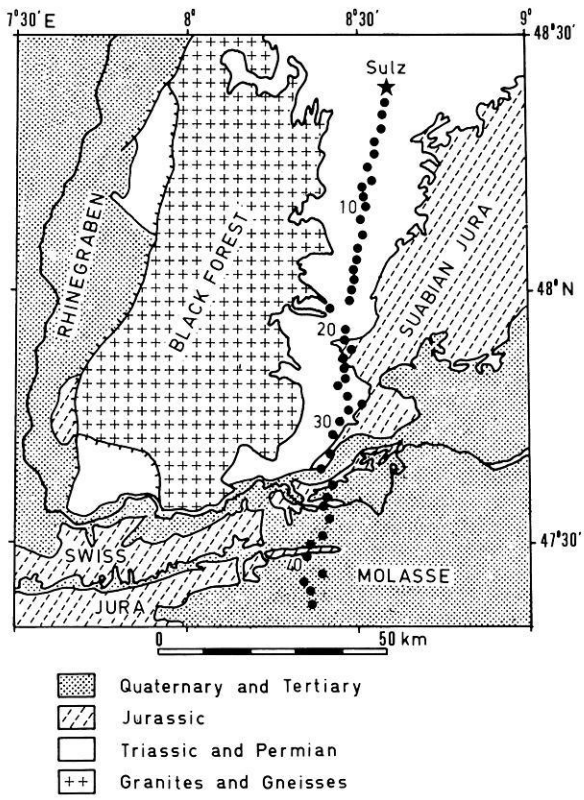

Fig. 1. Geological map with shotpoint (star) and station locations (dots) of profile Sulz-south. Stations are numbered consecutively from north to south. Information regarding the crust-mantle transition applies to the range between stations 10 and 20

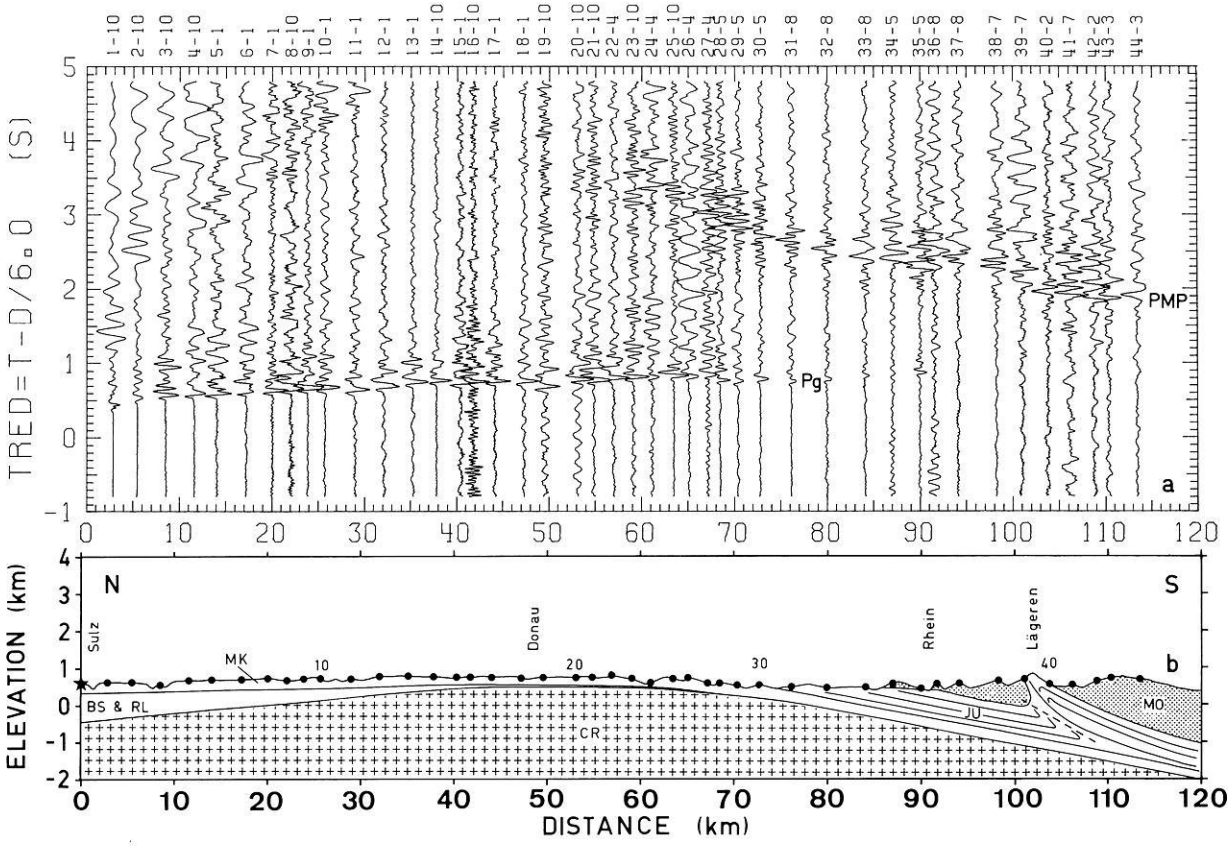

Fig. 2. a Trace-normalized, vertical component record section, with 32-Hz anti-aliasing filter. Numbers above each trace indicate station and shot. **b** Topography and geological crossection along profile Sulz-south. Vertical exaggeration: 4 times. MK-Muschelkalk and Keuper, BS = Bundsandstein, RL = Rotliegendes, MO = Molasse, JU = Jura, CR = Crystalline basement

(Boigk and Schoeneich, 1968; Breyer, 1956; Buechi et al., 1965; Lemcke et al., 1968; Schneider, 1980), it is possible to construct a rough cross-section of the sedimentary structure and of the topography of the crystalline basement (Fig. 2b). Thus the sediment-basement boundary is characterized by an up-dip over the first 40 km and a down-dip beyond about 60 km. In the north, the surficial upper Triassic sediments (Keuper and Muschelkalk) are underlain by a thick wedge of lower Triassic and Permian deposits (Buntsandstein and Rotliegendes). In the south, these Triassic sediments are covered by a layer of Jurassic limestones and by two Molasse basins, which are separated by the Jurassic outcrop of the Laegeren, the easternmost part of the folded Jura mountains.

Data Acquisition and Processing

All shots were recorded on FM-magnetic tape instruments of the MARS type (Berckhemer, 1970). Except for three stations with FS-60 seismometers (nos. 5, 6, 7 in Figs. 1 and 2), all instruments were equipped with three-component MARK L-4 seismometers with a natural frequency of 2 Hz. Timing was accomplished by recording the coded DCF radio-transmitted time signal along with the shots. The signals were digitized electronically with a sampling rate of about 400 Hz, using the recorded pilot frequency of the MARS instruments to drive the digitizer. After decoding the time signal, determining the exact sampling rate and removing possible spikes from the seismograms, the signals were filtered with a digital, zero-phase, 32-Hz low-pass filter, and the sampling rate was reduced to 100 Hz. During plotting of the record sections, an additional recursive, zero-phase band-pass filter could be applied to the data, to enhance various features of the signals. Figure 2a presents the vertical component data, filtered only with the 32-Hz anti-aliasing filter. The amplitudes are trace-normalized, but gain factors, which are calculated for each seismogram by the plot program, allow the determination of absolute ground velocity.

Since the distance range over which individual shots were recorded overlap with each other, amplitudes could be normalized to the same charge size where necessary. Because of poor recordings, some sites were occupied more than once.

Upper Crust

The *Pg* travel-time and amplitude data have already been presented in the context of a general discussion of amplitude modelling of the *Pg*-phase (Banda et al., 1982). In the resulting model (Fig. 4), the crystalline basement is characterized by a zone with a velocity gradient of 0.074 km/s/km between 1 and about 6 km depth, followed by a second zone with a weaker gradient (0.02 km/s/km) down to a depth of about 8 km.

Usually, several models can be made to fit the travel-time data by compensating changes in basement velocities with changes in sediment structure. However, in this case,

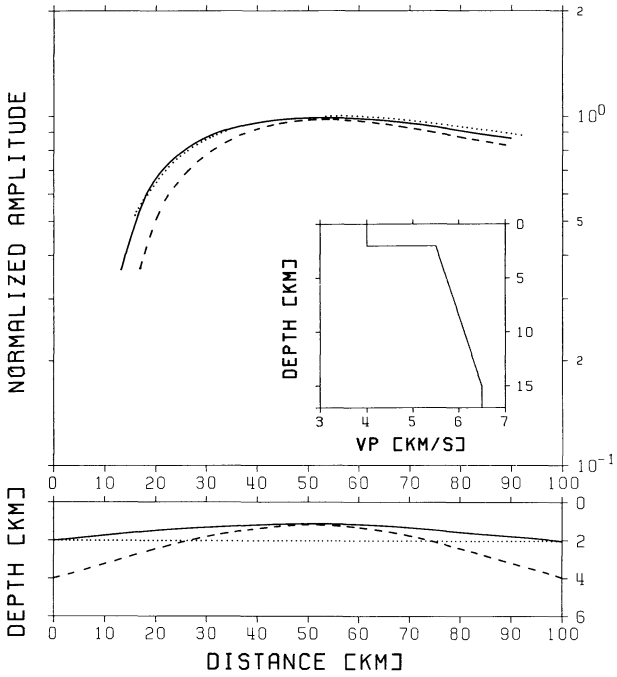

Fig. 3. Ray amplitudes (top) for model PG11, shown in the inset, with three different interface shapes (bottom)

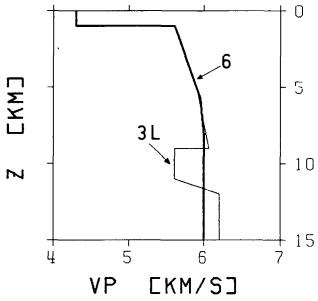

Fig. 4. Velocity-depth models of the upper crust. Model 6 is from Banda et al. (1982) with slightly lower sedimentary velocity. Model 3L corresponds to the synthetic seismograms in Fig. 5b

the overall topography of the sediment-basement boundary is fairly well known and for the first 70 km the sediments are less than 1 km thick, so that the travel-time data alone strongly constrains the range of possible velocity gradients in the upper crust. The calculation of additional models showed that reducing the upper gradient to less than 0.06 km/s/km, or increasing it beyond 0.085 km/s/km would no longer be compatible with the measured travel times. Beyond about 70 km, the thickness of the sedimentary layer increases and its velocity is not well known: thus sediment velocities can be varied in order to compensate for travel-time effects due to different velocities in the lower of the two gradient zones mentioned before. As shown by model 3 in Fig. 14 of the paper by Banda et al. (1982), a stronger gradient, extending over a sufficiently large depth range, produces a second amplitude increase beyond about 65 km. From those results it follows that the lower gradient is not greater than 0.04 km/s/km and that the velocity at the bottom of the gradient zone, which is reached at a depth between 8 and 10 km, is less than 6.1 km/s.

The amplitude calculations were performed using the reflectivity method developed by Fuchs (1968) and Fuchs and Müller (1971), as modified by Kind (1978). For computational reasons the models with curved interfaces, derived from the combination of borehole data (Fig. 2b) and ray-trace modelling (Banda et al., 1982), had to be approximated by a flat-layered model. In order to estimate the error introduced into the amplitude calculations by this simplification, several test-models were calculated using program RAY81, written by V. Červený and I. Pšenčík, which, based on asymptotic ray-theory, allows for laterally inhomogeneous models (Červený et al., 1977; Červený, 1979). Figure 3 shows the amplitude-distance curves for the *Pg*-phase, computed by this method for a flat-layered model, for a model with interfaces curved like those beneath Sulz (Fig. 2b) and for one with stronger curvature. The flat-layered model corresponds to PG11 in the paper by Banda et al. (1982, Fig. 8). The discrepancies between these curves and those calculated with the reflectivity method by Banda et al. are due to the inability of asymptotic ray-theory to account for wave-effects occurring at the top and bottom of the gradient zone. However, asymptotic ray-theory correctly accounts for geometrical spreading, so that the effects of different model geometries on the amplitudes can be compared with each other. The results displayed in Fig. 3 demonstrate that, in the case of the Sulz profile, shooting up-dip over the first 40 km and down-dip beyond about 60 km has only a negligible effect on the amplitudes of the *Pg*-phase. Consequently, all the synthetic seismograms discussed below were computed with the reflectivity method.

Structure of the Middle Crust

Looking at refraction data alone, evidence for a velocity discontinuity or inversion in the upper or middle crust should manifest itself as one or two intermediate reflections between the *Pg* and *PMP* arrivals. Although some of the records from Sulz contain large amplitudes in this interval, phases are very difficult to correlate over more than a few traces (see Fig. 2). Only in the distance range between 70 and 90 km does there seem to be a coherent arrival at about 0.5 s after the *Pg* (Fig. 5a).

In order to explain the travel time of these arrivals, several ray-trace models were calculated, both with a positive velocity discontinuity and with an inversion. A simple positive velocity jump below the gradient zone cannot simultaneously account for the large delay of this phase and for the close distance from the shot. Therefore a low-velocity layer had to be taken into consideration. The most satisfactory fit of the travel time data and of the *Pg* amplitudes was obtained with model 3L, which is characterized by a velocity drop from 6.06 to 5.6 km/s at a depth of 9 km and a gradual increase to 6.2 km/s between 11 and 12 km (Fig. 4). The synthetic seismograms corresponding to model 3L, in the distance range between 65 and 95 km, are displayed in Fig. 5b. A comparison of the amplitudes of the reflection from the bottom of the low-velocity layer (denoted by *PcP*), relative to those of the *Pg*, between data and synthetics shows a significant discrepancy. While in the calculated seismograms the amplitude ratios of *PcP* to *Pg* reaches a value greater than 2 at a distance of 85 km, in the data the maximum is about 1, and occurs at distances as short as 76 km.

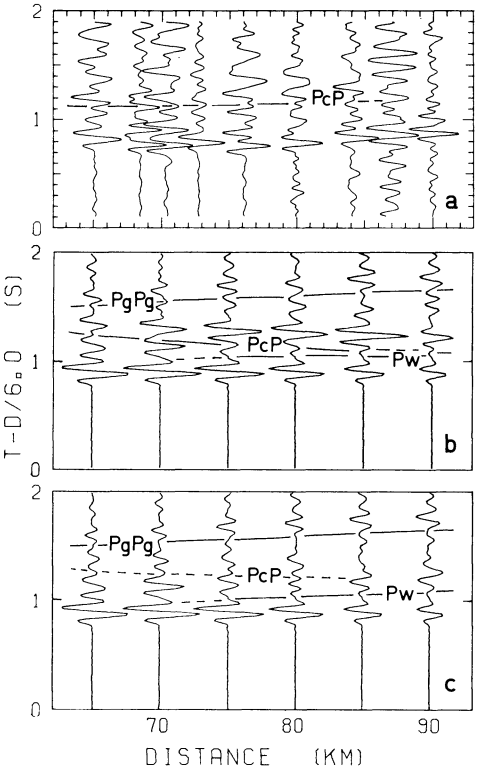

Fig. 5. a Vertical component records, trace normalized, 4–16 Hz band-pass filtered, showing possible reflections from the lower edge of an upper-crustal low-velocity layer (*PcP*). **b** Synthetic records for model 3L (Fig. 4) with Q=100 for the sediments and 500 for the rest of the crust. **c** Synthetic records for model 3L (Fig. 4) with Q=50 and V_p=5.4 km/s in the low-velocity zone. *PgPg*: *Pg* phase reflected once at the surface. *PcP*: reflection from the bottom of the low-velocity layer. *Pw*: interference head-wave, or "Whispering gallery phase" (see Červený et al., 1977). The amplitudes of the synthetic records are multiplied by distance and correspond to ground velocity

Changes in the gradient at the base of the inversion or a decrease of the velocity inside the channel will not simultaneously reduce the amplitudes of the *PcP* phase and move the maximum to shorter distances (Braile and Smith, 1975; Müller and Mueller, 1979). Braile (1977) showed that lowering the Q-value in the channel will significantly decrease the amplitudes of the *PcP* reflection. The synthetic seismograms presented so far were all calculated with a constant Q of 500 for the crystalline crust underlying a sedimentary layer with Q equal to 100. The seismograms shown in Fig. 5c correspond to a model similar to the previous one, except for the velocity and Q-value of the inversion zone, which were lowered to 5.4 km/s and 50, respectively. Under these conditions, the *PcP* reflection is so weak that it cannot be distinguished from the multiple reflections and conversions of the *Pg* phase within and beneath the sediments. Though other more realistic Q-values in the range between 50 and 500 are likely to be compatible with the observations, the data is not judged to be distinctive enough to allow a simultaneous determination of both velocity and Q structure in the middle crust. Indeed Banda et al. (1982) showed a synthetic seismogram example for a model without any discontinuity or inversion beneath the upper crustal gradient zone, in which the multiply reflected and converted phases within the sedimentary layer produce amplitudes similar to those observed here (see also Fig. 9). Accurate modelling would also require a better knowledge of Q in the sediments: anelastic attenuation is likely to influence the strength of the sedimentary reverberations as well.

Though the synthetic seismograms contain reflections from the upper boundary of the low-velocity layer, which closely follow the *Pg*-arrivals between 35 and 55 km (not shown here), they are also masked by sedimentary effects. Similarly, the reverberations observed in the data at these distances (Fig. 2a) do not exhibit the character of a distinct arrival, so that they cannot be relied upon for a unique interpretation.

Thus, based on the evidence from this data alone, it is not possible to conclusively resolve the problem of the possible existence of a low velocity layer in the middle crust below the Sulz profile. Resorting, therefore, to the criterion which favours the simpler of those models that are not in conflict with the data, further calculations were performed assuming a constant velocity of 6.0 km/s for the middle crust (model 6 in Fig. 4).

Crust-Mantle Transition

While the *Pg*-phase is quite impulsive, the *PMP* has a fairly well correlated precursor, and is followed by a coda of irregular reverberations. Moreover, the *PMP*-precursor appears to be frequency dependent: it is enhanced in the high-pass record section, while it is only faintly visible in the low-pass section (see Fig. 6). In fact, spectral analysis shows that the main signal energy lies in the frequency range between 2 and 16 Hz. However, the spectrum of the *Pg*-phase peaks around 8 Hz, while the reflection from the crust-mantle boundary often contains a maximum around 4 Hz and another one around 10 Hz. Since two different shots were recorded in the distance range in which the *PMP* and its precursor are observed, it is very unlikely that this signal character is merely a source effect. Thus the structure of the lower crust appears to be selective with regard to the frequency of the seismic signals returned from it.

Davydova (1972) classified possible crust-mantle transitions into three different types: first order discontinuities, transition zones with smoothly or stepwise increasing velocities, and transition zones consisting of lamina-like velocity inversions. Her conclusions indicate that a detailed analysis of the frequency dependent dynamic properties of the reflected wave field can provide criteria for distinguishing between the different types (see also Davydova et al., 1972).

In the course of studying the wave field generated by various models of the crust-mantle transition (Moho) with the aid of synthetic seismograms, Fuchs (1970) showed how a laminated upper mantle structure could produce a ringing signal following the main reflection, which is quite similar to that observed on some of the records in Fig. 6a. An alternative explanation for these reverberations is illustrated by the synthetic seismograms in Fig. 7. In this case the phases following the main *PMP* reflection are entirely due to multiple reflections and conversions of the *PMP* within the sedimentary layer both beneath the shotpoint and the receivers. Assuming a sedimentary layer which is thinner than the 2 km chosen for this example and whose thickness is not constant over the entire profile, the individual arrivals will merge and interfere with each other, thus producing an irregular pattern of vibrations, similar to those observed

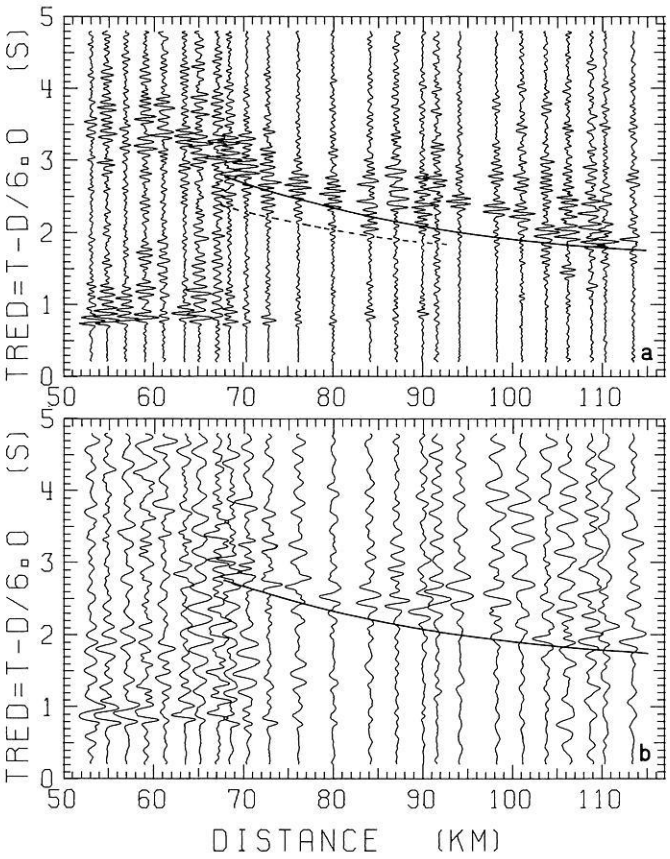

Figs. 6a and b. Trace normalized, vertical component record sections with **a** 10–24 Hz band-pass filter and **b** 5 Hz low-pass filter. Continuous travel-time curves correspond to the wide-angle reflections from the crust-mantle transition of the models in Fig. 9, calculated with a ray-trace program (Gebrande, 1976) taking into account the curved sediment-basement boundary shown in Fig. 2. The dashed curve indicates the *PMP*-precursor (*PrP*)

in the data. This shows that reverberations from an upper mantle lamellation will be at least partially masked by this sedimentary effect. Additional upper crustal discontinuities will of course increase these interference phenomena even further. Since the length of the profile is insufficient to detect a first arrival refracted from the upper mantle (*Pn*), the data cannot contribute anything to the knowledge of the structure below the Moho. Thus, following the reasoning of Edel et al. (1975), a constant upper mantle velocity of 8.0 km/s was adopted for further calculations.

Fuchs (1970) as well as Braile and Smith (1975) presented several synthetic record sections for various models of the Moho. From a comparison with these, it is obvious that the Sulz data cannot be modelled with a simple first order velocity discontinuity at the Moho, but that some kind of transition zone must be introduced in the lower crust. Figure 8 shows portions of synthetic record sections computed for various kinds of transitions. As shown by Fuchs (1968), the behaviour of a velocity gradient can be approximated by a stack of thin layers with stepwise increasing velocities. If, however, these layers are not thin enough relative to the wavelength of the incident signal, and if the velocity contrast between each layer is too strong, they will generate individual reflections. The faint precursors in the first seismograms of model 2 in Fig. 8 are due to subcritical reflections from the individual layers, while the large amplitude phase corresponds to the wide-angle reflection from the velocity jump at the bottom of the transition zone. The amplitude of the precursors relative to the main phase will increase as the number of steps in the gradient zone is decreased, but, at the same time, the reverberation-like character observed in the data is lost. This is illustrated by models 5 and 9 in Fig. 8. By extending the gradient zone all the way to the mantle without a larger velocity jump at the Moho, as in model 10, the individual velocity jumps are more pronounced than in model 2, which increases the amplitude of the reverberations. The velocity

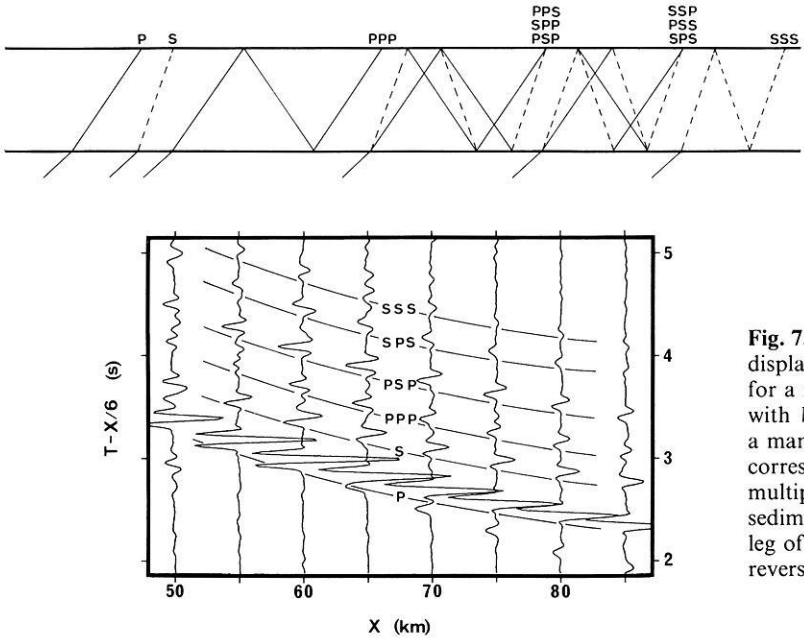

Fig. 7. Synthetic seismograms (vertical) component, ground displacement, amplitudes multiplied by distance) calculated for a model consisting of a 2 km thick sedimentary layer, with $V_p = 4.5$ km/s, over a basement with $V_p = 6.0$ km/s and a mantle with $V_p = 8.0$ km/s at 23 km depth. The first phase corresponds to *PMP*, while all subsequent arrivals are multiple reflections and conversions of the *PMP* within the sediments. Each letter of the phase identification denotes one leg of the ray-paths in the sedimentary layer. Note the phase reversals of the reflections at the surface

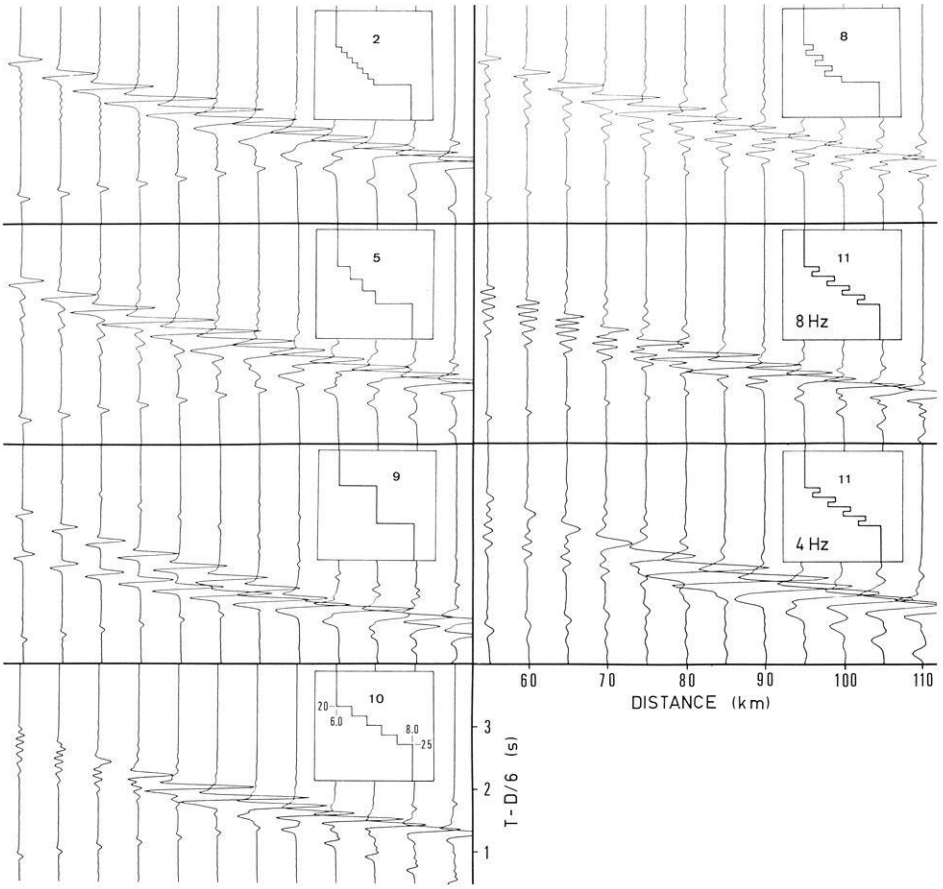

Fig. 8. Synthetic seismograms (vertical component, ground displacement, amplitudes multiplied by distance) for various models of the lower crust. The transition zone extends from a depth of 20 to 25 km, and the velocity increases from 6.0 to 8.0 km/s in all models. The phase with an apparent velocity of 5.5 km/s, visible in the lower part of each quadrant, is a numerical effect corresponding to the lower limit of the phase-velocity window used in the reflectivity program

contrast and consequently also the precursor amplitudes will be even larger if the individual steps include velocity inversions.

Reflections from a transition zone consisting of a series of lamellae with alternating high and low velocities have been investigated theoretically by Fuchs (1968; 1969; 1970), who demonstrated the dependance of the signal character both on frequency and angle of incidence. In order to account for high-frequency precursors before the lower-frequency *PMP* phase observed along a seismic refraction profile in France, Fuchs and Schulz (1976) proposed a model of the crust-mantle transition consisting of a thin high-velocity lamella over a zone of strong velocity gradient. However, in these cases, the large velocity discontinuity at the top of the transition zone would produce precursor amplitudes larger than observed under Sulz. A structure in which the velocity of the lamellae increases with depth will produce reverberations whose amplitudes increase more gradually. This is illustrated by models 8 and 11 in Fig. 8. The amplitude of the precursor relative to the main reflection depends on the size of the individual velocity jumps. The synthetic seismograms, corresponding to model 11, were also calculated for a signal with a dominant frequency of 4 Hz instead of 8 Hz (Fig. 8). A comparison of the two record sections shows a frequency dependent behaviour similar to that observed in the low- and high-pass filtered record sections in Fig. 6. At lower frequencies, the precursors, corresponding to subcritical reflections from the lamellae, are significantly attenuated, and the whole transition zone appears more like a smooth gradient, producing a single strong phase whose amplitude decreases rapidly towards shorter distances. A similar frequency dependent behaviour will of course also be produced by a step-model without inversions, such as model 10 in Fig. 8 (see Fuchs, 1968). On the basis of the preceding discussion, we must conclude that the crust-mantle boundary beneath Sulz is a transition zone several kms thick, and that it does not consist of a smooth gradient, but of a series of velocity jumps or even of a series of lamina-like inversions.

In order to fit the Sulz *PMP*-travel-time data as well as the amplitudes, the linear velocity increase from one step or lamella to the next in models 10 or 11 had to be modified. The data requires a thicker transition zone with velocities increasing slowly at the top and more rapidly below. This resulted in the models 10s and 11s, presented in Figs. 9a and b, together with the corresponding synthetic seismograms. For comparison, the recorded seismograms in the same distance range are reproduced in Fig. 9c.

A qualitative comparison alone already indicates that the recorded signal is better matched by the lamella-structure. Only the most significant part of the record section is shown: beyond about 85 km, the precursors interfere with the emerging *Pn* phase, while at distances shorter than 68 km, they are masked by strong signal generated noise (see Figs. 2 and 6). Some records at the shorter distances lack a clearly defined *PMP*-arrival, so that for a quantitative evaluation not all amplitudes could be measured. While both the *PMP* amplitude-distance curves and the *Pg* to *PMP* amplitude ratios of the step- and of the lamella-model fit the data equally well, the *PrP* to *PMP* amplitude ratios

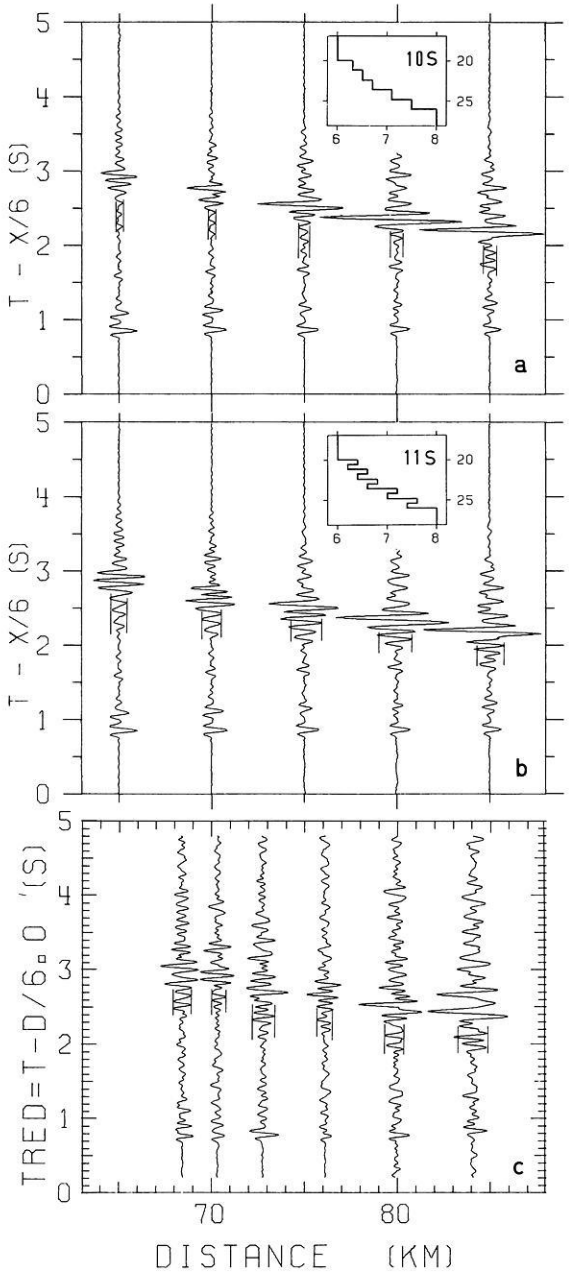

Figs. 9a and b Synthetic seismograms (vertical component, ground velocity, dominant frequency 8 Hz) for the crust-mantle transitions shown in the insets. Upper crustal model used corresponds to model 6 in Fig. 4 (see Table 1). Note the phases between *Pg* and *PMP*-precursors, caused by multiples and conversions of *Pg* within and beneath the sediments. **c**. Vertical component records, 4–16 Hz band-pass filtered. Vertical lines indicate amplitude of precursors as plotted in Fig. 11. Amplitudes of synthetics and data are scaled by multiplying with distance

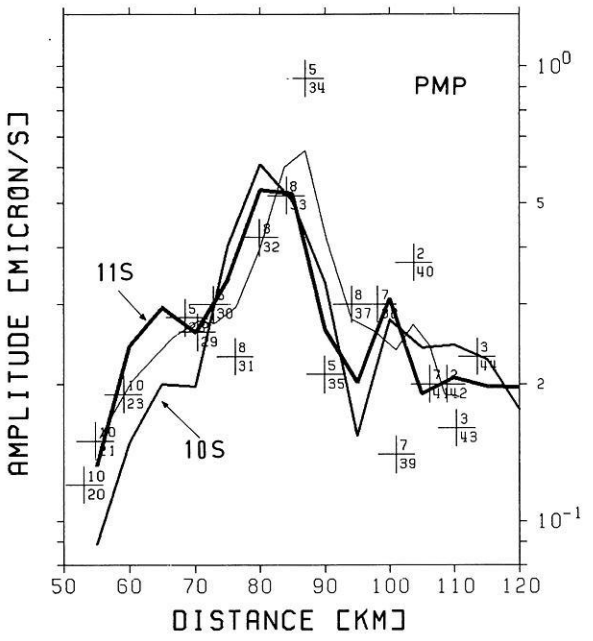

Fig. 10. Maximum amplitudes of *PMP* main phase (crosses with shot number above and station number below) from 4–16 Hz band-pass filtered records. Thin curve corresponds to smoothed data. Thick curves correspond to the step- (10S) and lamella-model (11S) in Fig. 9

allow one to distinguish between the two models (Figs. 10 and 11). In the distance range over which the precursors are clearly identifiable, the lamella-model fits the data very well, while the step-model deviates by about a factor of 3. Since errors due to faulty instrument gains or to differences in local site responses have no effect on the amplitude ratios this deviation can be regarded as significant. From this it follows that, of the models discussed here, a laminated crust-mantle transition explains the observations best.

We have also investigated two of the models consisting of a series of step-like gradients proposed by Edel et al. (1975) for the southern Black Forest: while the travel times can be made to fit the Sulz data quite accurately, the amplitudes of the *PMP* and its precursor do not match the observations sufficiently well. Indeed, it is likely that a quantitative amplitude interpretation of Edel's data might reveal that the *PMP*-precursors visible in some of his record sections are more adequately explained by some kind of lamination similar to that proposed here.

Conclusions

This study is the result of a combined interpretation of travel-times and amplitudes. For the computation of synthetic seismograms, the reflectivity method has proven to be a very powerful tool. For models with only slight lateral variations, its limitation to flat homogeneous layers is not serious and is amply compensated by its ability to correctly simulate the wave nature of seismic signals. However, computational techniques based on asymptotic ray-theory, which allow for lateral heterogeneities, are a valuable tool for estimating the effect of the flat-layer approximation.

The influence of the frequency content of the source on the ability to resolve finer structural details has already been pointed out by others (see Spudich and Orcutt, 1980, for an excellent review of computational techniques and interpretational pitfalls), but is all too often forgotten when comparing results from different investigations, in particular from sea- and land-shots.

A further important and often neglected consideration to be taken into account when interpreting the deeper crustal structure is the influence of the sediments or surficial weathered layer. Small variations in sedimentary structure or velocity can produce significant travel-time effects, while

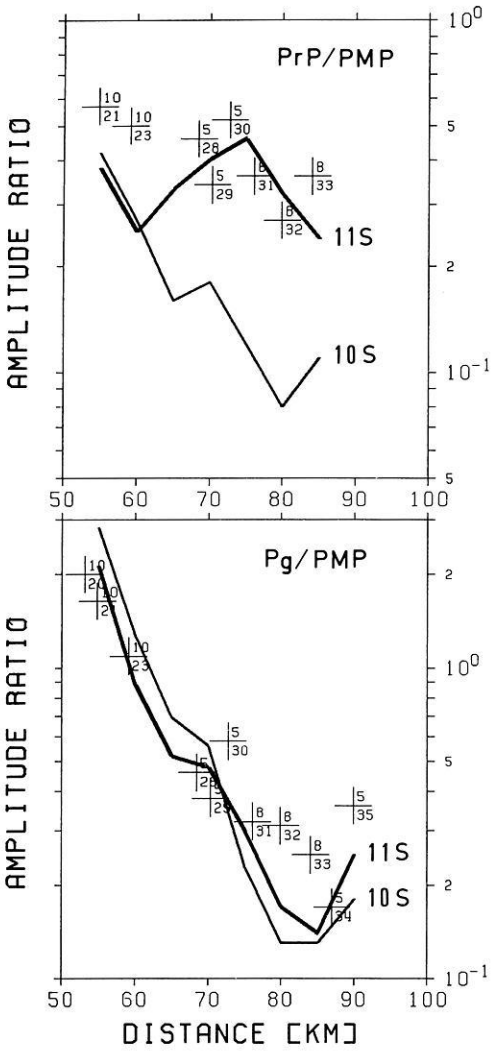

Fig. 11. Amplitude ratio of *PMP*-precursor (*PrP*) to *PMP* main phase (*top*) and amplitude ratio of *Pg* to *PMP* (*bottom*). Crosses correspond to data (shot numbers above, station numbers below). Continuous curves correspond to the step- (10S) and the lamella-model (11S) in Fig. 9

multiple reverberations and *P-S* conversions between the top of the basement and the Earth's surface can mask phases from deeper discontinuities. For example, without independent information from borehole data about the dip of the sediment-basement boundary under Sulz, the travel-time interpretation would have resulted in a significantly different velocity gradient in the upper crust, and it would have been difficult to achieve an agreement with the amplitude data. A more accurate knowledge of the sedimentary structure at the southern end of the Sulz-profile would put stronger constraints on the lower part of the upper crustal gradient as well as on the shape of the velocity increase in the transition zone above the Moho. For accurate synthetic seismogram modelling, it would furthermore be desirable to obtain reliable Q-values for the sediments.

Figure 12 shows the complete velocity-depth model proposed for the crustal structure along the eastern margin of the southern Black Forest (see also Table 1). Its main features are a strong gradient in the upper crust and a crust-mantle transition zone composed of a series of lamella-shaped velocity inversions.

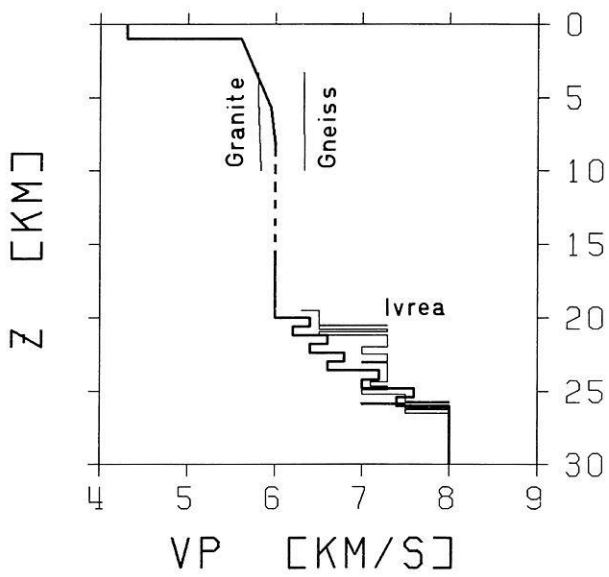

Fig. 12. Velocity-depth model for SULZ 11S with results of laboratory measurements by Kern and Richter (1981) and velocity profile through the Ivrea body, after Hale and Thompson (1982)

Table 1. Parameters of model SULZ 11S

Lower limit of layer (km)	Layer thickness (km)	V_p (km/s)	Number of layers	Gradient (km/s/km)
1.0	1.0	4.3	2	0.0
5.7	4.7	5.6 –5.95	7	0.074
8.2	2.5	5.95–6.0	4	0.02
20.0	11.8	6.0	2	0.0
20.6	0.6	6.4	1	0.0
21.2	0.6	6.2	1	0.0
21.8	0.6	6.6	1	0.0
22.4	0.6	6.4	1	0.0
23.0	0.6	6.8	1	0.0
23.6	0.6	6.6	1	0.0
24.2	0.6	7.2	1	0.0
24.8	0.6	7.0	1	0.0
25.4	0.6	7.6	1	0.0
26.0	0.6	7.4	1	0.0
30.0	4.0	8.0	1	0.0

Unambiguous evidence for or against a discontinuity or low-velocity zone in the middle crust could not be found from this data alone. However, it is possible that near-vertical reflection data would reveal additional structure at depths of 10–12 km: in the Rhinegraben, echoes with a travel-time of about 4 s have been interpreted as reflections from the top of a low-velocity layer in this depth range (Mueller et al., 1969; 1973), which could extend to the east below the Black Forest.

The upper crustal gradient is exceptionally well constrained by information about the basement topography (boreholes) and by travel-time as well as amplitude data. From the geological setting (Fig. 1), it is to be expected that the granites and gneisses of the Black Forest extend to greater depths below the Sulz profile. For comparison, the top part of two velocity-depth curves from laboratory measurements by Kern and Richter (1981) for a granite and a gneiss sample, assuming a geotherm corresponding

to a warm continental crust (Theilen and Meissner, 1979) are included in Fig. 12. Only the lower part of the gradient zone, below a depth of about 5 km, is similar to these measurements. They were performed on dry and unfractured samples. The much stronger gradient found in the uppermost part of the crust could imply that fractures and water content, including pore pressure, have to be taken into account when interpreting the elastic parameters of the basement, even at depths down to about 5 km (Nur and Simmons, 1969; Mueller, 1977).

The evidence for the lamination in the lower crust is based on a quantitative comparison of the amplitudes of the *PMP* and its precursors with those of theoretical seismograms. It also correctly accounts for the observed traveltimes and for the frequency dependent nature of the reflections from the crust-mantle transition. In addition the Moho-depth of 26 km, corresponding to the distance range between 30 and 50 km from the shot point, agrees perfectly with the results extrapolated from the Rhinegraben by Edel et al. (1975).

Several other authors have postulated a laminated crust-mantle transition zone before, based partly on near-vertical reflection data (Meissner, 1967; 1973; Fuchs, 1969; Clowes and Kanasewich, 1970; Davydova, 1972; Bartelsen et al., 1982). The present study provides additional independent evidence for the existence of such a structure. As presented here, it corresponds closely to a laminated Conrad discontinuity extending all the way to the Moho, in analogy to the high-velocity tooth in the lower crust, discussed by Mueller (1977).

While the vertical extent of the transition zone and the general velocity increase with depth is directly supported by the data, the regularity of the lamella thickness and the strength of the inversions is largely an arbitrary artifact. Whether an existing lamella-structure is seen or not is in part a function of the wavelength of the recorded signals, which in turn puts certain constraints on the average thickness of the individual lamellae. However, the real structure is probably much less regular than suggested by this model. Moreover, nothing can be said about the lateral extent of such a structure.

Hale and Thompson (1982) review a number of seismic reflection lines which show evidence of lamination in the lower continental crust, and note that such a structure seems to be relatively discontinuous. In addition, taking the lithologic sequence of the Ivrea-Verbano zone (northern Italy) as a model of the lower crust, they computed a synthetic vertical incidence reflection seismogram, which shows striking similarities to recorded ones. For comparison, this model has been superimposed on the Sulz-model in Fig. 12. Though the two models differ in detail, the laminated sequence of high- and low-velocity layers is common to both.

Acknowledgements. This project was possible thanks to D. Emter (Schiltach) who advised us of the quarry blasts and recorded the shot-times. His helpful suggestions regarding the sedimentary structure in the northern part of the profile are also gratefully acknowledged. E. Banda, H. Scriba and L.W. Braile contributed with numerous helpful discussions. M. Grieder's maintainance and improvements of the recording instruments were essential to the success of the measurements. Thanks are due to D. Gajewski, B. Guggisberg and V. Červený for advice on computing the ray-theoretical amplitudes. St. Mueller critically read the manuscript and added several suggestions for improvement.

References

Banda, E., Deichmann, N., Braile, L.W., Ansorge, J.: Amplitude study of the *Pg* phase. J. Geophys., **51**, 153–164, 1982

Bartelsen, H., Lueschen, E., Krey, Th., Meissner, R., Schmoll, H., Walter, Ch.: The combined seismic reflection-refraction investigation of the Urach geothermal anomaly. In: The Urach Geothermal Project, pp. 247–262. Stuttgart: Schweizerbart 1982

Berckhemer, H.: MARS66 – a magnetic tape recording equipment for deep seismic sounding. Z. Geophys. **36**, 501–518, 1970

Boigk, H., Schoeneich, H.: Die Tiefenlage der Permbasis im nördlichen Teil des Oberrheingrabens. In: Graben Problems, J.H. Illies and St. Mueller (eds.), pp. 45–55. Stuttgart: Schweizerbart 1968

Braile, L.W., Smith, R.B.: Guide to the interpretation of crustal refraction profiles. Geophys. J. R. Astron. Soc. **40**, 145–176, 1975

Braile, L.W.: Interpretation of crustal velocity gradients and Q structure using amplitude-corrected seismograms. In: The earth's crust, Am. Geophys. Union Mon. **20**, 427–439, 1977

Breyer, F.: Ergebnisse seismischer Messungen auf der süddeutschen Grosscholle besonders in Hinblick auf die Oberfläche des Varistikums. Z. d. Dt. Geol. Ges. **108**, 21–36, 1956

Büchi, U.P., Lemcke, K., Wiener, G., Zimdars, J.: Geologische Ergebnisse der Erdölexploration auf das Mesozoikum im Untergrund des schweizerischen Molassebeckens. Bull. Ver. Schweiz. Petrol. -Geol. u. -Ing. **32**, 82, 7–38, 1965

Červený, V.: Ray Theoretical seismograms for laterally inhomogeneous structures. J. Geophys. **46**, 335–342, 1979

Červený, V., Molotkov, I.A., Pšenčík, I.: Ray method in seismology. Prague: Charles University Press 1977

Clowes, R.M., Kanasewich, E.R.: Seismic attenuation and the nature of reflecting horizons within the crust. J. Geophys. Res. **75**, 6693–6705, 1970

Davydova, N.I.: Possibilities of the DSS technique in studying properties of deep-seated seismic interfaces. In: Seismic properties of the Mohorovicic discontinuity, Davydova, N.I., ed.: pp 4–22. Moscow: Izdatel'stvo Nauka 1972. English translation from: National Technical Information Service, U. S. Dept. of Commerce, Springfield, Va, 1975

Davydova, N.I., Kosminskaya, I.P., Kapustian, N.K., Michota, G.G.: Models of the earth's crust and M-boundary. Z. Geophys. **38**, 369–393, 1972

Edel, J.B., Fuchs, K., Gelbke, C., Prodehl, C.: Deep structure of the Southern Rhinegraben area from seismic refraction investigations. J. Geophys. **41**, 333–356, 1975

Emter, D.: Ergebnisse seismischer Untersuchungen der Erdkruste und des obersten Erdmantels in Südwestdeutschland. Diss. Univ. Karlsruhe, 1971

Emter, D.: Seismic results from Southwestern Germany. In: Explosion seismology in Central Europe, P. Giese, C. Prodehl, A. Stein, eds.: pp. 283–289. Berlin, Heidelberg, New York: Springer 1976

Fuchs, K.: Das Reflexions- und Transmissionsvermögen eines geschichteten Mediums mit beliebiger Tiefenverteilung der elastischen Moduln und der Dichte für schrägen Einfall ebener Wellen. Z. Geophys. **34**, 389–413, 1968

Fuchs, K.: On the properties of deep crustal reflectors. Z. Geophys. **35**, 133–149, 1969

Fuchs, K.: On the determination of velocity depth distributions of elastic waves from the dynamic characteristics of the reflected wave field. Z. Geophys. **36**, 531–548, 1970

Fuchs, F., Müller, G.: Computation of synthetic seismograms with the reflectivity method and comparison with observations. Geophys. J. R. Astron. Soc. **23**, 417–433, 1971

Fuchs, K., Schulz, K.: Tunneling of low-frequency waves through the subcrustal lithosphere. J. Geophys. **42**, 175–190, 1976

Gebrande, H.: A seismic-ray tracing method for two-dimensional inhomogeneous media. In: Explosion seismology in Central Europe, P. Giese, C. Prodehl, A. Stein, eds.: pp. 162–167. Berlin, Heidelberg, New York: Springer 1976

Hale, L.D., Thompson, G.A.: The seismic reflection character of the continental mohorovicic discontinuity. J. Geophys. Res. **87**, 4625–4635, 1982

Jentsch, M., Bamford, D., Emter, D., Prodehl, C.: A seismic-refraction investigation of the basement structure in the Urach geothermal anomaly, Southern Germany. In: The Urach Geothermal Project, pp. 231–245. Stuttgart: Schweizerbart 1982

Kern, H., Richter, A.: Temperature derivatives of compressional and shear wave velocities in crustal and mantle rocks at 6 kbar confining pressure. J. Geophys. **49**, 47–56, 1981

Kind, R.: The reflectivity method for a buried source. J. Geophys. **44**, 603–612, 1978

Lemcke, K., Buechi, U.P., Wiener, G.: Einige Ergebnisse der Erdölexploration auf die mittelländische Molasse der Zentralschweiz. Bull. Ver. Schweiz. Petrol. -Geol. u. -Ing. **35**, 87, 15–34, 1968

Lohr, J.: Die seismischen Geschwindigkeiten in der Ostschweiz. Bull. Ver. Schweiz. Petrol. -Geol. u. -Ing. **34**, 85, 29–38, 1967

Lohr, J.: Die seismischen Geschwindigkeiten der jüngeren Molasse im Ostschweizerischen und Deutschen Alpenvorland. Geophys. Prosp. **17**, 111–125, 1969

Meissner, R.: Exploring deep interfaces by seismic wide angle measurements. Geophys. Prosp. **15**, 598–617, 1967

Meissner, R.: The 'Moho' as a transition zone. Geophys. Surveys **1**, 195–216, 1973

Mueller, S.: A new model of the continental crust. In: The Earth's crust, Geophysical Monograph 20, pp. 289–317. Washington, D.C.: Am. Geophys. Union 1977

Mueller, S., Peterschmitt, E., Fuchs, K., Ansorge, J.: Crustal structure beneath the Rhinegraben from seismic refraction and reflection measurements. Tectonophys. **8**, 529–542, 1969

Mueller, S., Peterschmitt, E., Fuchs, K., Emter, D., Ansorge, J.: Crustal structure of the Rhinegraben area. Tectonophys. **20**, 381–391, 1973

Müller, G., Mueller, S.: Travel-time and amplitude interpretation of crustal phases on the refraction profile Delta-W, Utah. Bull. Seismol. Soc, Am. **69**, 1121–1132, 1979

Nur, A., Simmons, G.: The effect of saturation on velocity in low porosity rocks. Earth Planet. Sci. Lett. **7**, 183–193, 1969

Prodehl, C., Ansorge, J., Edel, J.B., Emter, D., Fuchs, K., Mueller, S., Peterschmitt, E.: Explosion-seismology research in the Central and Southern Rhinegraben – A case history. In: Explosion seismology in Central Europe, P. Giese, C. Prodehl, A. Stein, eds.: pp. 313–328. Berlin, Heidelberg, New York: Springer 1976

Schneider, T.R.: Geologische Beilage, Sondiergesuche an die Gemeinden Weiach und Bachs, ZH, NSG11, NSG12. Baden: NAGRA 1980

Spudich, P., Orcutt, J.: A new look at the seismic velocity structure of the oceanic crust. Rev. Geophys. Space Phys. **18**, 3, 627–645, 1980

Theilen, F., Meissner, R.: A comparison of crustal and upper mantle features in Fennoscandia and the Rhenisch shield, two areas of recent uplift. Tectonophys. **61**, 227–242, 1979

Received September 29, 1982; Revised version December 8, 1982
Accepted December 13, 1982